Conformity of aluminum thin films deposited onto micro-patterned silicon wafers by pulsed-laser deposition, magnetron sputtering, and CVD

Anne-Lise Thomann, Constantin Vahlas, Lyacine Aloui, Diane Samelor, Amaël Caillard, Nurhul Shaharil, Romuald Blanc, Eric Millon

DOI: 10.1002/cvde.201106936

Conformity of Aluminum Thin Films Deposited onto Micro-Patterned Silicon Wafers by Pulsed Laser Deposition, Magnetron Sputtering, and CVD**

By *Anne-Lise Thomann*,* *Constantin Vahlas*, *Lyacine Aloui*, *Diane Samelor*, *Amael Caillard*, *Nurhul Shaharil*, *Romuald Blanc*, and *Eric Millon*

Complex materials, exhibiting a cocktail of properties, are currently needed for many applications. In this context, new requirements arise in terms of materials processing, such as the synthesis of sub-micrometer objects, or the coating and functionalization of complex surfaces of powders, porous materials, or micro-patterned devices. Depending on the requirements, the aim may be to duplicate the original design of the surface, or to modify it (filling of holes etc.). Physical vapor deposition (PVD) and CVD are promising techniques for the deposition of thin films on such substrates. In order to compare the ability of various deposition techniques to coat complex surfaces, a micro-patterned silicon wafer has been developed. In the present work, aluminum thin films are deposited on this model substrate by two PVD techniques; pulsed laser deposition (PLD) and magnetron sputtering (MS), and by metal-organic (MO)CVD. Scanning electron microscopy (SEM) is performed in order to determine the microstructure and study the thickness conformity.

Keywords: Aluminum, Complex surface, Conformity, Micro-patterned substrate, Plasma magnetron sputtering, Pulsed laser deposition

1. Introduction

PVD and CVD are widely used to process thin films and coatings in various application fields such as microelectronics, optics, fuel cells, photovoltaics, cutting tools, etc. With the development of microsystems, and the general requirements for tailor-made materials, deposition has to be performed on complex substrates, some of them being composed of micrometer patterns such as trenches, holes, blocks. Depending on the desired final design, the base pattern may be reproduced or, on the contrary, modified. Thus, it is of particular interest to study the ability of various deposition techniques either to maintain unchanged the surface design (thickness conformity of the thin film) or to change their shape (filling of trenches).

According to the authors' experience, investigation of conformity of films deposited on patterned substrates by academic groups occurs most often through relationships with microelectronics industries or R&D centers in the frame of commonly led projects. Such investigations are made on dedicated substrates which are of particular interest for the material and the application to be developed. This situation presents three drawbacks; (a) the architecture is not unique, (b) it is not possible to follow up the evolution of the characteristics of the films as a function of the pattern dimensions, (c) the substrates are not easily available to a wider public. With the aim of investigating phenomena occurring during deposition on complex-shaped surfaces, a model silicon substrate was developed in the frame of the French research laboratory group (CNRS Groupement de Recherche 2008), entitled ''Mécanismes de dépôts par voie gazeuse sur des Surfaces à Géométrie Complexe'' (SurGeCo, http://surgeco.grenoble-inp.fr/). SurGeCo is dedicated to the investigation of deposition mechanisms of films onto complex substrates such as powders, porous materials, and micro-patterned surfaces. Investigation of thickness uniformity and of morphology of thin films deposited on such patterns is expected to provide information which is potentially useful for e.g., a) modeling the deposition process, b) modeling the nucleation and growth mechanisms (thus providing deeper understanding of the involved mechanisms), and c) comparing different processing techniques. These patterned wafers are available for any research purpose.

The present work is concerned with the latter point, with Al deposition being selected as a case study. Al thin films are

[*] Dr. A.-L. Thomann, Dr. A. Caillard, N. Shaharil, R. Blanc, Dr. E. Millon
Laboratoire GREMI, CNRS/Université d'Orléans, 14 rue d'Issoudun BP 6744, 45067, Orléans cedex 2 (France)
E-mail: anne-lise.thomann@univ-orleans.fr
Dr. C. Vahlas, L. Aloui, Dr. D. Samelor
Université de Toulouse, CIRIMAT/INPT, 4 allée Emile Monso BP 44362, 31030 Toulouse cedex 4 (France)

[**] This work was performed in the frame of the Research Group (GdR) "SURfaces de GEométrie COmplexe" (SURGECO) funded by CNRS. Karine Blary and the IEMN Lille are acknowledged for the fabrication of the patterned substrates.

deposited onto micro-patterned Si wafers by PLD, MS, and MOCVD. In the two PVD techniques the flux of condensing atoms is expected to be anisotropic, the main direction being perpendicular to the substrate surface, however modification of the processing conditions (pressure, incidence angle, substrate bias voltage) is known to affect the surface diffusion process, which impacts on the homogeneity of the growing film. In contrast to PVD techniques, the surface reaction-limited regime of MOCVD yields conformal coverage of the substrate, but the conformity is sometimes balanced by the resulting rougher microstructures. This often occurs in MOCVD of metals where activation energies for the nucleation of the film are larger, resulting in almost discontinuous films composed of large grains.

Thus, although the main objective of the present contribution is the comparison of the features of Al films deposited by three different techniques (under conventional deposition conditions), it cannot be dissociated from an insight into the morphology and microstructure of the films with respect to the experimental parameters. In the present work, for the three techniques under investigation, these parameters were varied in experimentally accessible ranges. Microstructure and thickness of the Al thin films were determined using SEM performed on cross-sections of the micrometer-size trenches. Results are presented by plotting conformity factors (defined below) versus the aspect ratio (depth/width) of the trench.

2. Methods

Micro-patterned Si substrates are obtained from plasma etching and electron lithography of a SiO_2 mask which was designed and fabricated by the Institute of Electronics, Microelectronics, and Nanotechnology (IEMN), Lille. The patterns were transferred onto Si wafers with three etching depths; 0.6 μm, 1 μm, and 1.3 μm. Each wafer can be cleaved into 20 samples of area 1 cm^2 containing 80 patterns of various shapes and lateral dimensions. Available patterns are; trenches with apertures from 0.5 μm to 10 μm, circular and square holes and blocks with typical width ranging from 0.5 μm to 3 μm. The distance between each pattern is also different (ranging from 0.5 μm to 10 μm), in order to study the possible effect of the periodicity on the film features. The shapes and dimensions of the patterns were varied in the full ranges accessible with both mask fabrication processes.

Holes and blocks are not strictly aligned in order to have a chance to get a cross-sectional view when the sample is cloven. The variety of patterns on such a substrate permits the study, in a single deposition run, of the film uniformity and structure on trenches of five different aspect ratios (between 0.13 and 2.6) and on five types of patterns.

Figure 1 shows two SEM images of a part of the as-received, micro-patterned Si wafers. 1 μm depth and 1.5 μm width trenches separated by 0.5 μm walls are visible in the cross-sectional image (lower micrograph of Figure 1).

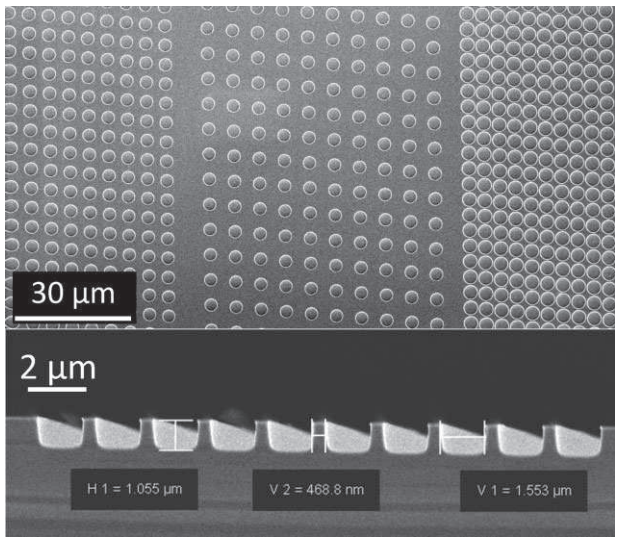

Fig. 1. Top view of circular blocks (upper micrograph) and cross-sectional view of trenches (lower micrograph) of as-received micro-patterned Si substrate.

Domains containing different densities of circular blocks are presented in the top view (upper micrograph of Figure 1).

In the present work, only the trench domain of the substrate was exploited. Figure 2 schematically illustrates the pattern of Al films deposited on the top, bottom, and side walls of a trench. Indicated are the positions where the thickness T_x of the film (T_t, T_b, and T_s, respectively) is measured. The conformity of the films at the bottom (C_b) and the side walls (C_s) can be defined according to Equation 1 (adapted from the literature[1,2]).

$$C_x = \left(1 - \frac{T_t - T_x}{T_t}\right) * 100 \quad (1)$$

These coefficients allow the qualification of the film uniformity taking the top thickness as reference. C_b and C_s quantify the deviation of the thickness at various locations of the pattern. Equation 1 is another way to express the well-known step coverage[3] independently of the absolute thickness value. Since on the model substrate all patterns are present, this definition is mainly useful to compare different deposits. To precisely study the film uniformity,

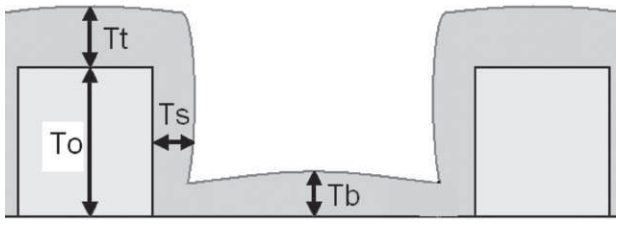

Fig. 2. Schematic of an Al film coating a trench with an etched depth T_0.

statistical analysis of the film thickness on a single pattern was proposed by Krumdieck et al.[4] With the aim of comparing deposition techniques, we rather chose to investigate the film thickness at defined locations of the pattern (bottom and side) for numerous aspect ratios available on the model substrate. C_b provides insight into the ability of the incoming atoms to enter within the trench and coat the bottom, and C_s is related to the directionality of the atom flux. These parameters will be studied as a function of the aspect ratio of the trenches.

3. Results

3.1. PLD

In PLD, the interaction regime with a metal surface depends on the laser beam pulse time duration.[5,6] When the pulse lasts several tenths of nanoseconds (ns), thermal interaction occurs; the laser energy is absorbed by the conduction electrons which collide with the metal lattice atoms. This induces heating of the surface, and, for sufficiently high fluence (energy per square centimeter), vaporization is initiated. In ns PLD, a melting bath is present at the vaporized surface from which droplets of liquid are ejected and travel to the substrate where they are deposited within the growing film.[7] Al vaporization by UV laser irradiation is moderately efficient because UV light absorption by the surface, at the initial step of the process, is prevented by the high reflectivity (92%). To overcome such drawbacks, a solution may be to turn to shorter pulse laser beams. Indeed, when the interaction time is in the range of picoseconds (ps) and lower, other phenomena, such as multiphoton absorption become predominant.[8] This mechanism leads to a fast electron ejection. The resulting Coulombian interaction between electrons and metal lattice ions induces an explosive ejection of material. This may balance low UV light absorption efficiency and increase the deposition rate. Furthermore, when the thermal ejection mechanism is avoided, deposition of droplet-free thin films is expected.

In the present work it was not possible to deposit droplet-free Al films using the ps laser. This indicates that, even in the ps time scale, non-negligible thermal effects occur at the surface of aluminum, and that a molten bath is formed during the interaction with the laser.[5,6] Because the growth rate of films processed by ps laser was too low, deposition was performed using the ns laser. In Figure 3, SEM images of an Al thin film, deposited by PLD at 13 J cm^{-2} during 3 h, are presented. An intermediate fluence was selected so that droplet formation was, at best, avoided while keeping a reasonable deposition rate.

In the upper micrograph of Figure 3, a dense and homogeneous film is observed coating the bottom and top of the trench, due to the deposition of Al atoms that have been transported in the plasma plume. In the background, a big droplet can be observed, revealing the transport of the liquid phase from the target to the substrate. This cross-section reveals a fine structure consisting of small columns the orientation of which is different on the side walls than on the surfaces parallel to the substrate. The orientation of the columnar grains is illustrated by the dotted lines in the upper micrograph of Figure 3. Such a columnar morphology is typical of growth by PVD techniques.[9] Orientation of the columns can give some insight into the growth conditions, and this is discussed in the following paragraph.

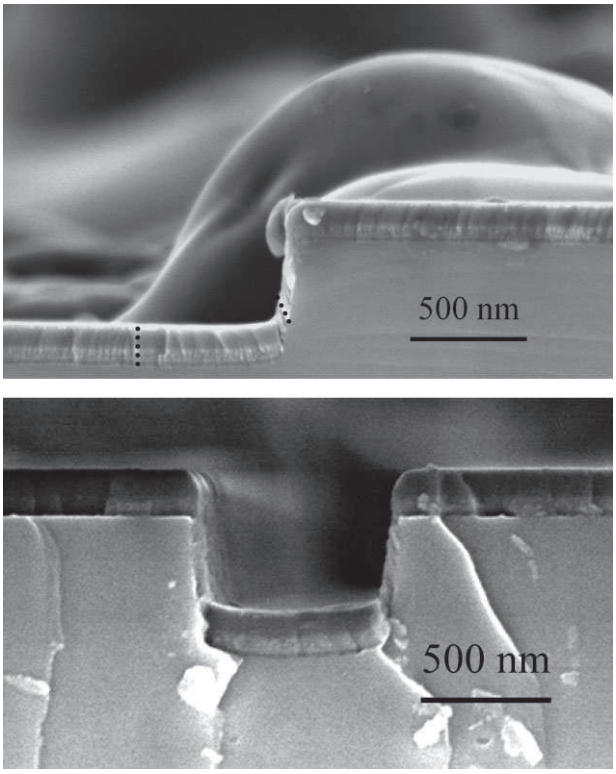

Fig. 3. Al film deposited by ns PLD with a 13 J cm^{-2} laser fluence during 3 h. Side of a trench showing the homogenous part of the deposit and a droplet in the background. Dotted lines indicate the column orientation at the bottom and at the flank (upper micrograph). Coating of a trench (lower micrograph).

As already mentioned, PLD is not suitable for the synthesis of Al thin films, however investigation of the homogeneous part of the film reveals that the film thicknesses at the top and at the bottom are comparable, whereas that on the side walls is very thin. The conformity coefficients (bottom, C_b and side, C_s) of the Al PLD film were found to be independent of the aspect ratio. The bottom conformity is excellent (C_b values close to 100%) whereas the side conformity is poor (C_s never exceeds 35%).

3.2. MS

Whatever the deposition conditions, MS Al films are composed of well-defined and close-packed columns. This structure is characteristic of thin film growth by PVD at low

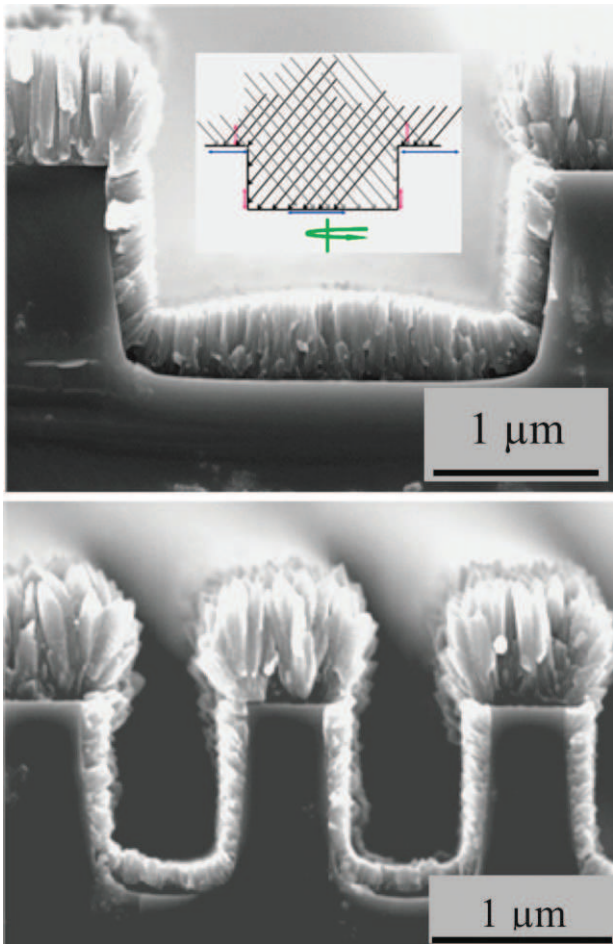

Fig. 4. Cross-sectional SEM images of sample PCref. The cartoon illustrates the orientation and penetration of the incoming Al flux when the substrate is rotating.

substrate temperature[9–11] and is shown in the micrographs of Figure 4 for sample PCref.

It can be noticed that the column characteristics such as width, height, and orientation are different at the bottom, at the side, and on top of the trench. Columns at the top and bottom are perpendicular to the substrate plane despite the fact that the substrate is tilted 38° with respect to the target normal. Under these conditions, and at low deposition temperature, the structure zone model predicts that the columns should be tilted.[9,12] The lack of tilt is due to the rotation of the substrate resulting in a mean flux perpendicular to the surface, as is schematically illustrated in Figure 4. On the trench side, due to the shadowing effect, the substrate rotation has no influence on the orientation of the columns which are tilted 30° with respect to the normal. This is in good agreement with experimental results on Al thin films reported in the literature.[13]

SEM images in Figure 4 reveal that the film conformity widely depends on the aspect ratio. When the aspect ratio is high, the growth at the trench top induces a shadowing effect which prevents the atom flux from penetrating inside the pattern. The thickness at the bottom is thus smaller than on the top, but close to that on the side walls (lower micrograph of Figure 4). For lower aspect ratios, arriving atoms are allowed to penetrate into the pattern and the thickness at the bottom increases. Moreover, because of the target rotation, overlapping of fluxes of opposite direction occurs, which enhances the deposition rate at the center of the bottom surface, resulting in a curved profile of the film thickness. This behavior is demonstrated in the upper micrograph of Figure 4.

The evolution of bottom and side conformities, as a function of the aspect ratio of the trenches, is given in Figure 5. Both C_b and C_s increase with decreasing aspect ratio. C_b is close to 100% at 0.1 aspect ratio, but C_s never exceeds 50%. Results for different MS films are similar although slight differences are observed among those processed under different conditions. An increase in pressure induces an increase in the collisions between ejected atoms and gas, improving the isotropy of the incoming flux.[14] This behavior should result in more uniform films, as indeed observed on C_b evolution, but not on that of C_s (PC2 sample). Similarly, glancing angle should

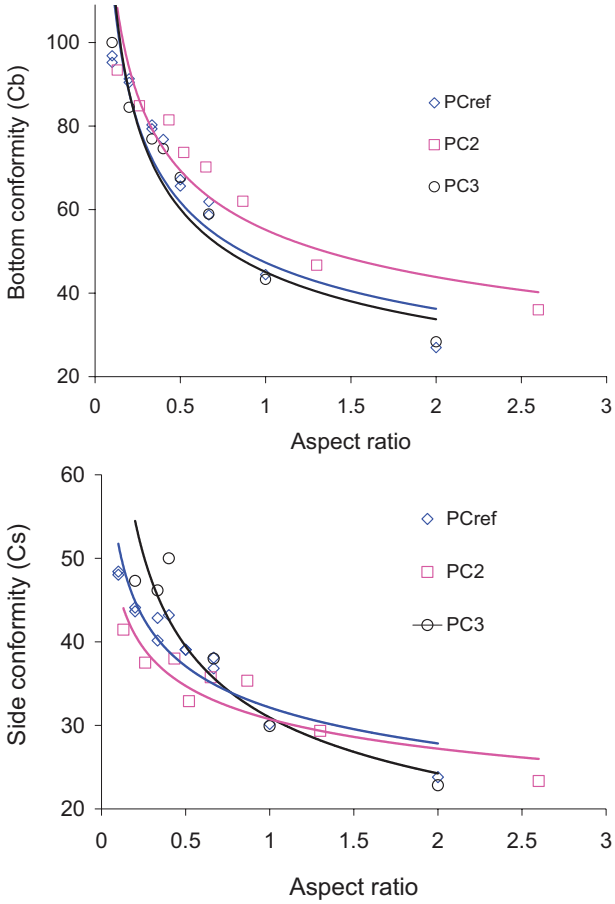

Fig. 5. Bottom (C_b) and side (C_s) conformity of MS-processed Al thin films, as a function of the aspect ratio of the trenches.

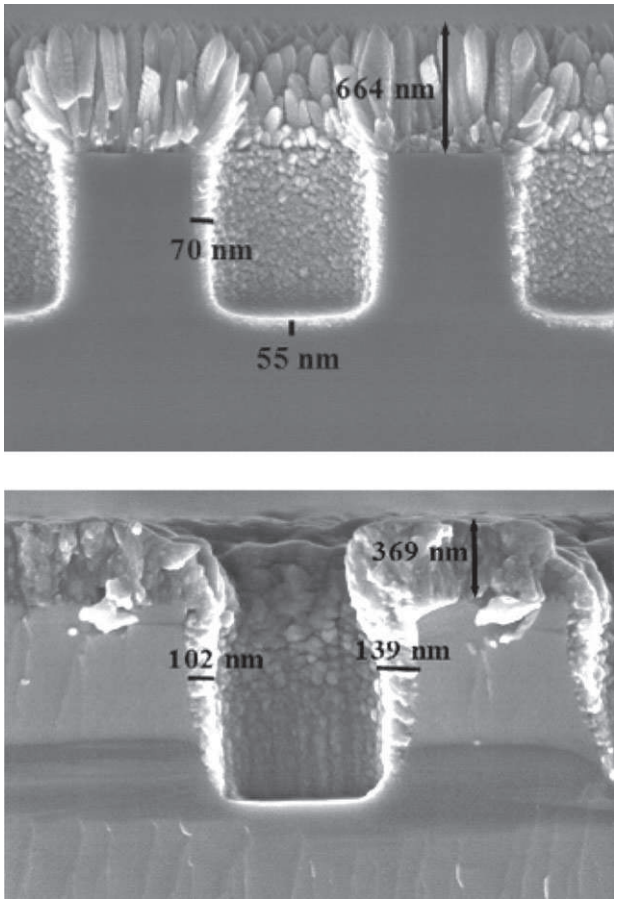

Fig. 6. Comparison of the morphology of MS-processed Al film without (upper micrograph) and with (lower micrograph) substrate bias voltage.

enhance the shadowing effect and thus reduce deposition rate on the side and bottom walls, which is not observed in the graphs (PC3 sample). It appears that the selected variations of pressure and incidence angle are not extended enough to affect the uniformity of the films.

Figure 6, shows two cross-section micrographs of a biased substrate (PC 4 sample, lower micrograph) compared to PCref sample (upper micrograph). Biasing the substrate accelerates the argon ions present in the plasma, which then assist the deposition process. It is observed that the bias voltage affects film morphology. The film appears denser and the columns are partly destroyed. It is known that ion bombardment enhances film density[9] and this is observed in the present case, however it is difficult to know, from the limited number of experiments reported in the present work, if the modification of the morphology is rather due to the ballistic effect or to the local increase in temperature. Another result is that ion assistance of the deposition does not lead to an enhanced diffusion of the Al atoms inside the pattern as could be expected from collisions occurring between incoming atoms and ions. Consequently, the conformity is not improved when the substrate is biased.

3.3. MOCVD

A major concern of MOCVD-processed Al films is the often rough microstructure obtained due to the reluctance of Al to nucleate on silicon and silicon-based ceramic surfaces. This behavior has been extensively reported in the literature and has been faced, at least partially, through appropriate treatments of the involved surfaces (see the literature[15] and references therein). The nature of the Al precursor also influences the resulting film morphology. For example, it has been reported that films processed from dimethylethyl amine alane (DMEAA) present a significantly smoother microstructure than those processed from triisobutyl aluminum (TIBA), the latter probably being the most widely used metal-organic precursor of Al.[16]

The present experiments do not aim at optimizing the microstructure of the MOCVD-processed Al films. Instead, the starting point of the deposition conditions investigated (sample patSi-01) is the one recently adopted by the authors in the experimental and theoretical investigation of the MOCVD of Al from DMEAA on flat substrates. Figure 7 summarizes the mean (Ra) and peak-to-valley (Rz) roughness of the surface of the films, together with their crystallite size and their thickness, the latter being measured at the top surface (T_t). The Ra of film patSi-01 equals 20 nm, i.e., a comparable value to the one reported in the literature,[17] however Rz equals 0.67 μm, this value being significantly higher than that of Ra.

Figure 8 presents two-cross sectional SEM images, characteristic of samples processed under reference conditions (patSi-01, upper micrograph) and at low temperature, low precursor concentration (patSi-05, lower micrograph). Film patSi-01 presents a disordered structure, with the growth of large, independent grains which do not form a compact film. This is in agreement with the high value of Rz of this sample. This morphology was also observed for Al films deposited on polished bulk Al substrates and on SiC[15] and is characteristic of the previously mentioned trends concerning the competition between nucleation and growth of CVD-processed Al films.

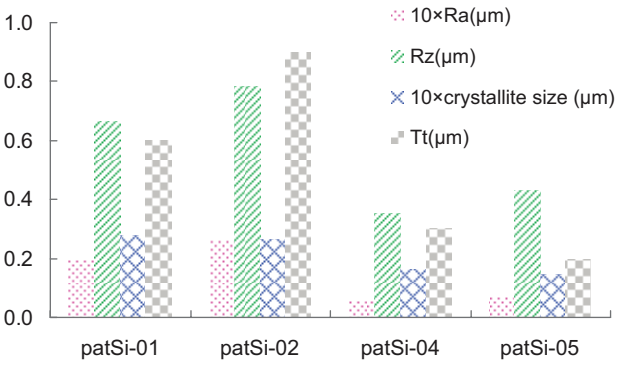

Fig. 7. Thickness (Tt), surface roughness (Ra, Rz) and crystallite size for the MOCVD-processed Al films.

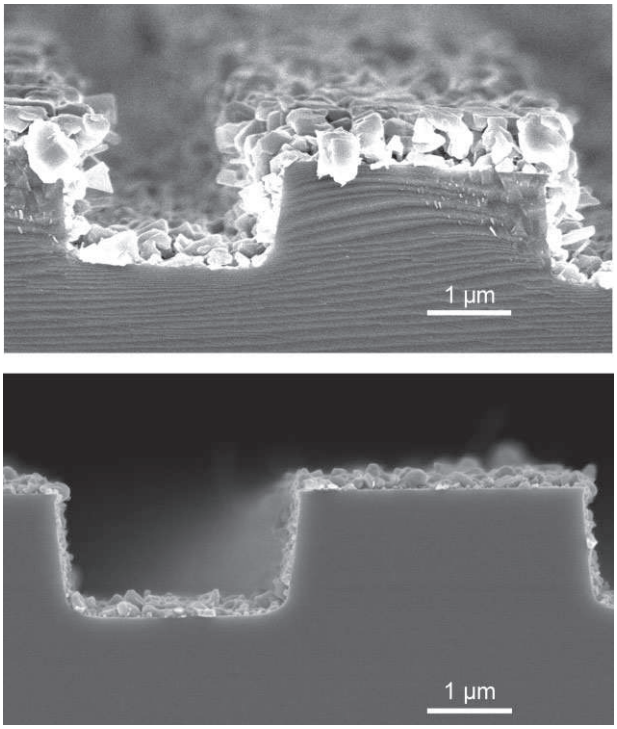

Fig. 8. Cross-sectional SEM images of samples patSi-01 (upper micrograph) and patSi-05 (lower micrograph).

Decreasing the deposition temperature (sample patSi-02) is expected to increase the supersaturation of the gas phase and, consequently the driving force for nucleation.[18] This trend should result in a smoother surface, while maintaining a high growth rate of the film according to the Arrhenius plot of the process.[19] The obtained film has the same thickness, indeed, but its roughness also remains similar to the former one (see Fig. 7). It is concluded that the variation in temperature is not enough to allow the expected behavior to occur. Further decrease of temperature was not attempted since it would result in significant decrease of the growth rate.

A second way to improve the granular morphology of the films was a decrease in the precursor concentration in the input gas with the aim of decreasing the growth rate, and consequently the size of the Al grains. The decrease in precursor concentration was achieved by decreasing the precursor flow rate through the increase of the operating pressure P_{tot}.[20]

Experiments patSi-04 and patSi-05 were performed under 5.82 kPa and 9.33 kPa, respectively, however decrease of the precursor concentration in the input gas also decreases the supersaturation, and consequently the driving force of the nucleation of Al on the substrate surface. For this reason, both experiments were initiated under standard pressure (1.33 kPa in the present study) for a short time period (4 min) prior to increasing the pressure for the remaining time of the experiments. The resulting values of *Ra* and *Rz* of both samples are four and two times smaller, respectively, from those of the previous runs (see Fig. 7). A similar trend holds for the size of the crystallites, which is reduced from *ca.* 270 nm in samples patSi-01 and patSi-02 to *ca.* 150 nm in samples patSi-04 and patSi-05. The simultaneous decrease of the roughness and of the size of the crystallites confirms the correlation of these trends with the increase in the operating pressure.

Observation of the lower micrograph in Figure 8 reveals that film patSi-05 presents a rather smooth surface with a film continuity which does not exist in the reference sample patSi-01. This is in agreement with the reduced values of roughness of this sample. It is worth noting that the mass gain of samples patSi-01 and patSi-05 is comparable (50 μg, and 40 μg, respectively), while there is a three fold decrease of the thickness of sample patSi-05 with regard to patSi-01 (0.6 μm and 0.2 μm, respectively). Despite the significant decrease of its thickness, film patSi-05 is continuous throughout the surface due to the presence of a continuous sublayer in the vicinity of the substrate. This result was demonstrated in the literature[15] for the MOCVD of Al by performing experiments under similar conditions to the present ones, and by decreasing the deposition time. All samples presented a continuous sublayer by the substrate with similar thickness. This comparison indicates that films processed using the two-step protocol involving high deposition pressure are less porous, and this is compatible with their reduced surface roughness.

The rough microstructure of the films patSi-01 and patSi-02 did not allow unambiguous determination of C_b and C_s. Figure 9 presents the evolution of C_b and C_s as a function of the aspect ratio of the trenches for both samples with the improved morphology, i.e., patSi-04 and patSi-05. In sample patSi-04 the values of C_b and C_s are 97% and 95%, respectively, at low aspect ratios. They gradually decrease to 81% and 65%, respectively, for an aspect ratio equal to 0.75. In sample patSi-05 the values of C_b and C_s are 99% and 95%, respectively at low aspect ratios, i.e., similar to those of sample patSi-04. Under these conditions, however, conformity is better maintained for higher aspect ratios, since at aspect ratios of 1 C_b and C_s remain higher than 95%. Despite the improved morphology of samples patSi-04 and patSi-05, the above values should be considered as a strong trend rather than a quantitative result. Nevertheless, they permit the conclusion that the applied two-step process, including increase of deposition pressure, has a beneficial effect on conformity, in addition to the improvement of the microstructure of the films.

4. Comparison of the Techniques

Samples PLD, PCref, and PatSi-05 are representative of PLD, MS, and MOCVD, respectively, and will be considered for the comparison of the microstructure and conformity of the Al films processed by the three techniques. As mentioned above, the obtained surface morphology and

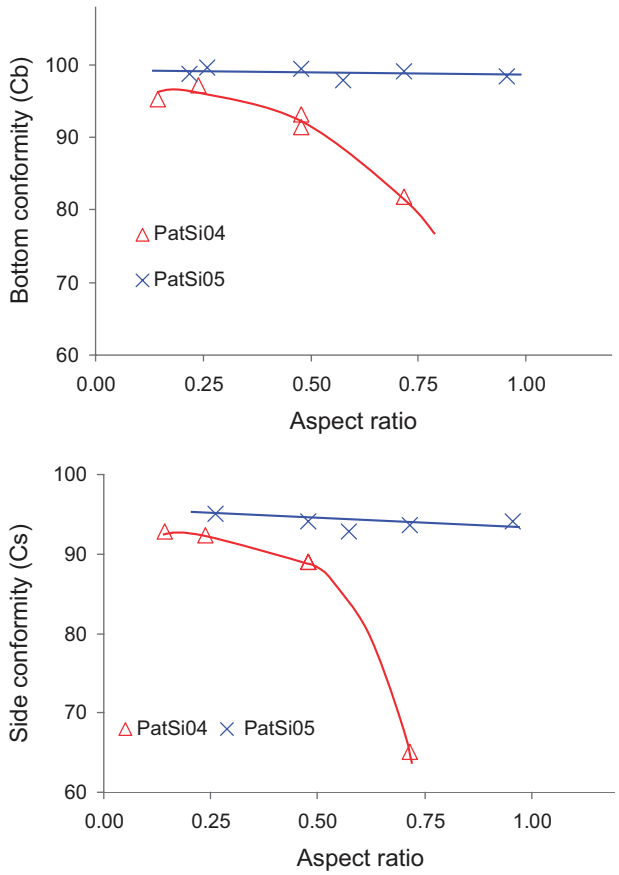

Fig. 9. Evolution of the bottom and side conformity as a function of the aspect ratio for samples patSi-04 and patSi-05. Lines are a guide to the eye.

in-depth structure are very different. MOCVD films were found to be rough, porous, and composed of large crystallites; MS films are formed of more or less packed columns (depending on the location, top, bottom or side); very dense films were grown by PLD.

Differences shown between MOCVD and PVD thin films are directly related to the growth mechanisms. In the former technique, the structure of the film depends on the outcome of the competition among a sequence of elementary steps occurring on the surface, namely adsorption of the precursor, reaction, diffusion, nucleation, and growth. In the present case the growth of the Al film is dominated by a mechanism involving adsorption of the DMEAA on the surface through the establishment of hydrogen bonds from the alane part, followed by dissociation and desorption of the amine, formation of H_2 on the surface, and desorption, leaving pure Al adatoms available for nucleation and growth.[21]

In the case of PVD methods, the growth is driven by the condensation mechanism, which is thermodynamically favorable. The film structure mainly depends on surface atomic diffusion, the efficiency of which is determined by the available energy (heated substrate, energy released by the incoming atoms or by energetic plasma particles interacting with the surface, etc.).

This relationship between deposition parameters (substrate temperature, pressure, etc.) has been widely studied by many authors[9,11,22] for PVD techniques via the structure zone model. With this tool it is possible to gain an insight into the deposition conditions from the film microstructure, and even to deduce the limiting mechanisms of the growth. The high density and featureless structure of the PLD films is typical of a high energy deposition process (zone II according to the literature[9]) and is due to the large kinetic energy carried by the Al atoms in the plasma plume expending in vacuum. The mean Al atom energy is of the order of tenths of eV, against several eV in MS.[9,23] In the latter case, the structure shown by SEM (see Fig. 4) corresponds to zone 1a or 1b in the literature,[9] and is formed when the mobility of adatoms is very low.

The bottom and side conformities are presented in Figure 10 for MS (PCref), MOCVD (patSi-05), and the PLD sample. From the graph it is clearly seen that only MS films have conformity varying with the aspect ratio. For instance, C_b value increases from 27% to 99% when the aspect ratio changes from 2 to 0.1. Even for the most favorable aspect ratios, the side conformity never exceeds 50%. This behavior indicates that the incoming atom flux is anisotropic, with a mean direction perpendicular to the substrate surface, and a characteristic distance of the trajectory distribution close to the pattern scale. The anisotropy was expected because of the low working pressure used which prevents scattering of the ejected atoms and thus furthers a directional flux. As a matter of fact, a perfectly perpendicular narrow flux (at the pattern scale) arriving at the surface is expected to induce deposition of films with the same morphological features whatever the aspect ratio; similar thickness at the bottom and at the top, limited deposition on the side walls. This is typically what is obtained on PLD films: C_b is close to 100% whatever the aspect ratio, and C_s is

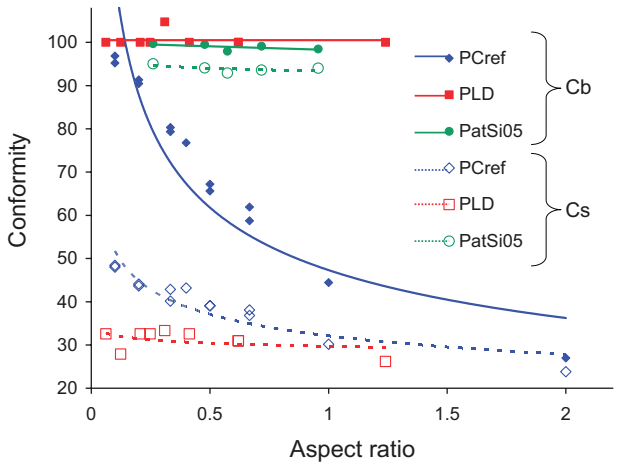

Fig. 10. C_b and C_s evolution versus the aspect ratio for Al thin films grown by MS (PCref), PLD, and MOCVD (pat-Si05).

very low (less than 35%). Compared to MS films, it is seen that the distribution of the atom flux trajectory is narrower. With PLD the original pattern shape is almost kept in the growing film. Figure 10 reveals that Al films with the best conformity (bottom and side) are obtained by MOCVD. This was expected in view of the surface reaction-limited mechanism prevailing in this case.

5. Conclusion

The conformity and structure of Al thin films, deposited by PVD (MS and PLD) and MOCVD onto micro-patterned silicon substrates, were investigated. Typical deposition conditions were used in all techniques without aiming to improve films characteristics by varying processing parameters and/or applying surface pretreatments. SEM observations performed around and inside trenches of various aspect ratios provided evidence of the film characteristics depending on the deposition technique.

Study of the microstructure showed that the Al films processed by MS, PLD, and MOCVD were columnar, dense, and rough, respectively. MS ensures high bottom conformity for low aspect ratios. Bottom and side conformity decrease with increasing aspect ratio. Bottom and side uniformity of PLD-processed films remain unchanged with varying the aspect ratio. Both conformity coefficients remain high in the entire aspect ratio range for MOCVD.

From these results it can be predicted that deposition by MOCVD under optimized conditions (to lower the roughness and enhance the density) will produce conformal deposits. With MS, depending on the coverage required for a given application, side and bottom thicknesses can be tailored by playing with the pattern dimensions. Finally, PLD allows a substrate to be coated, with the original pattern shape being transferred into the growing film.

Processing of films with predefined properties can be foreseen though the case-by-case selection of the most appropriate technique and the fine tuning of the deposition protocol. Investigations like the one presented here, can help in selecting the most appropriate solution to predefined requirements in applications such as metallurgical coatings on complex surfaces or microsystem design.

The present work revealed the utility of model substrates such as the micro-patterned Si used. Besides the qualitative comparison of techniques, they allow insight into the growth parameters. For example, the mean direction of the incoming particle flux can be determined from the column orientation in MS. To completely qualify the deposition conditions, comparison between experimental observations and simulation by numerical codes of film morphology in various patterns can be performed. This work is in progress in the frame of SurGeCo and is expected to provide insight into growth mechanisms.

6. Experimental

Material Synthesis: In PLD a laser beam is focused on an Al rotating target (2″, purity > 99%) with an angle of 45°. The target surface is vaporized under the laser beam action, and a dense and partly ionized metallic vapor is ejected. This plasma plume expansion (in vacuum) through the reactor is responsible for the transport of Al atoms to the substrate. In the present study, the temperature of the substrate is left floating. Before deposition, Si substrates were cleaned with dry air. Two kinds of UV laser beams with different pulse time durations and energy spatial distributions were tested; a Nd:YAG laser with a wavelength of 355 nm and a repetition rate of 10 Hz (40 ps, Gaussian energy distribution) and a KrF excimer laser with a wavelength of 248 nm and a repetition rate of 10 Hz (27 ns, ''top hat'' energy distribution). The use of both laser beams allows for a laser/metal interaction picosecond or nanosecond time range with different impact on the characteristics of the obtained films.

The chamber used for MS is dedicated to deposition onto large samples (15 cm × 15 cm) and equipped with two 4 inches magnetron cathodes. Only one was used in the present work. The Al target contained 2 at.-% Cu and 0.5 at.-% Fe, and was biased in the range 250–450 V. Typical current values were 0.5 A to 1 A. Argon pressure was varied from 0.5 Pa to 5 Pa. The substrate temperature was not regulated. Deposition was performed with an angle between substrate and target surfaces of 38°corresponding to standard conditions, and with an angle of 60°, corresponding to a glancing mode. Deposition was carried out at floating substrate bias or with the application of a RF bias voltage, which induces Ar^+ ion assistance of the condensing mechanism. Before deposition, Si substrates were cleaned with dry air. Table 1 presents the operating conditions for films processed by MS.

MOCVD was performed in a stagnant flow, cylindrical, vertical, stainless-steel reactor equipped with a plasma pretreatment system. The deposition chamber is made of a double envelope allowing monitoring of wall temperature through the circulation of thermally regulated silicon oil. Samples were positioned horizontally on a 58 mm diameter susceptor and were heated by a resistance coil gyred just below the surface of the susceptor. The input gas was distributed though a showerhead system containing a 60 mm diameter perforated plate.

The Si substrates were cleaned with hydrofluoric acid prior to introduction into the reactor. Immediately before deposition, the substrates were subjected for 30 min to plasma pretreatment with Ar/10% H_2 in conditions 120 kHz, 80 W, with the aim of removing the organic contaminants from the surface.

99% pure DMEAA (Epichem) was used (as received) as the Al precursor and placed in a stainless-steel bubbler. It was maintained at 281 K, corresponding to a saturated vapor pressure of 0.09 kPa, during the entire period of its service in order to avoid degradation [24]. 99.9992% pure N_2 (Air Products) was fed through two electropolished stainless-steel gas lines with VCR fittings. One line was used for bubbling through the Al precursor and the other for the dilution of the input gas. The flow rate of the diluting N_2 was 300 sccm, while the bubbling N_2 flow rate was 25 sccm. Assuming saturation of the gas phase, these conditions lead to an upper limit of the flow rate of DMEAA equal to 2 sccm under 1.33 kPa, 0.45 sccm under 5.82 kPa, and 0.26 sccm under 9.33 kPa.

C_b and C_s of Al films obtained from four experiments, performed under various conditions of pressure, temperature, and duration, were investigated. Table 2 gives details of the values of these processing parameters for each experiment. The conditions of sample patSi-01 were considered as standard in the present study. Those of the other samples were varied accordingly, targeting improvement of the microstructure and/or the conformity of the films.

Material Characterization: The microstructure of the films was analyzed with a SUPRA 40 (Zeiss) and a JSM6700F (Jeol) FEG-SEM. The roughness of MOCVD-processed films was determined using a Zygo MetroPro, New View 100 optical profilometer. Crystallite size was determined by application of the Scherrer equation, from the X-ray diffractograms obtained in a

Table 1. Operating conditions used in MS.

Sample code	Cathode voltage [pV]	Argon pressure [Pa]	Incidence angle	Substrate bias
PCref	375	1	Standard (38°)	floating
PC2	375	5	Standard (38°)	floating
PC3	375	1	Glancing (60°)	floating
PC4	375	1	Standard (38°)	50 W RF bias

Table 2. Operating conditions used in MOCVD experiments.

Sample code	P [kPa]	Deposition temperature [K]	Deposition time [min]
patSi-01	1.33	493	25
patSi-02	1.33	433	25
patSi-04	1.33 (the first 4 min) 5.82 (10 min)	433	15
patSi-05	1.33 (the first 4 min) 9.33 (10 min)	433	15

conventional θ-2θ configuration with a Seifert XRD 3000 TT diffractometer using CuKα radiation and fitted with a diffracted beam monochromator.

Received: May 17, 2011
Revised: September 15, 2011

[1] R. Huang, H. Wang, A. Qin, *Proc. SPIE* **2005**, 5753.

[2] S. Siriwonggrungson, M. Alkaisi, S. Krumdieck, *Surf. Coat. Technol.* **2007**, *201*, 8944.

[3] T. Kondo, Y. Sawada, K. Akiyama, H. Funakubo, T. Kigushi, C. Seki, M. H. Wang, T. Uchida, *Thin Solid Films* **2008**, *516*, 5864.

[4] S. Krumdieck, S. I. Baluti, L. Marcus, A. Peled, *Electrochem. Soc. Proc.* **2005**, *9*, 120.

[5] *Pulsed-Laser Deposition of Thin Films* (Eds: D. B. Chrisey, G. K. Hubler), J. Wiley, New York 1994.

[6] J. Perrière, C. Boulmer-Leborgne, R. Benzerga, S. Tricot, *J. Phys. D: Appl. Phys.* **2007**, *40*, 7069.

[7] *Pulsed Laser Deposition of Thin Films: Applications-Led Growth of Functional Materials* (Ed: R. W. Eason), John Wiley & Sons, New York 2007, ISBN: 0-471-44709-9.

[8] L. V. Zhigilei, *Appl. Phys. A* **2003**, *76*, 339.

[9] S. Mahieu, P. Ghekiere, D. Depla, R. De Gryse, *Thin Solid Films* **2006**, *515*, 1229.

[10] H. Savaloni, M. G. Shahraki, *Nanotechnology* **2004**, *15*, 311.

[11] J. A. Thornton, *J. Vac. Sci. Technol.* **1974**, *11*, 666.

[12] L. Abelmann, C. Lodder, *Thin Solids Films* **1997**, *305*, 1.

[13] S. Lichter, J. Chen, *Phys. Rev. Lett.* **1986**, *56*, 1396.

[14] T. P. Drüsedau, M. Löhmann, F. Klabunde, T.-M. John, *Surf. Coat. Technol.* **2000**, *133–134*, 126.

[15] C. Vahlas, P. Ortiz, D. Oquab, I. W. Hall, *J. Electrochem. Soc.* **2001**, *148*, 583.

[16] M. Delmas, C. Vahlas, *J. Electrochem. Soc.* **2007**, *154*, D538.

[17] A. N. Gleizes, V. V. Krisyuk, L. Aloui, A. E. Turgambaeva, B. Sarapata, N. Prud'homme, F. Senocq, D. Samelor, A. Zielinska-Lipiec, F. Dumestre, C. Vahlas, *ECS Trans.* **2009**, *25*, 181.

[18] C. Vahlas, E. Blanquet, *Thermochemistry of silicon LPCVD revisited with kinetic data*, MRS Symp. Proc. **1998**, *507*, 951.

[19] T. C. Xenidou, N. Prud'homme, C. Vahlas, N. C. Markatos, A. G. Boudouvis, *J. Electrochem. Soc.* **2010**, *157*, D633.

[20] C. Vahlas, B. Caussat, F. Senocq, W. L. Gladfelter, L. Aloui, T. Moersh, *Chem. Vap. Deposition* **2007**, *13*, 123.

[21] M. G. Simmonds, I. Taupin, et al., *Chem. Mater.* **1994**, *6*, 935.

[22] B. A. Movchan, A. V. Demchischin, *Fiz. Met. Metalbevd (USSR) (Phys. Met. Metallogr.)* **1969**, *28*, 653.

[23] A. L. Thomann, C. Boulmer-Leborgne, B. Dubreuil, *Plasma Sources Sci. Technol.* **1997**, *6*, 298.

[24] H. Matsuhashi, C.-H. Lee, T. Nishimura, K. Masu, K. Tsubouchi, *Mater. Sci. Semicond. Proc.* **1999**, *2*, 303.